Thermal energy recovery from chlorinated drinking water distribution systems: Effect on chlorine and microbial water and biofilm characteristics

Zhou, Xinyan; Ahmad, Jawairia Imtiaz; van der Hoek, Jan Peter; Zhang, Kejia

DOI
10.1016/j.envres.2020.109655

Publication date
2020

Document Version
Final published version

Published in
Environmental Research

Citation (APA)
Zhou, X., Ahmad, J. I., van der Hoek, J. P., & Zhang, K. (2020). Thermal energy recovery from chlorinated drinking water distribution systems: Effect on chlorine and microbial water and biofilm characteristics. *Environmental Research*, *187*, Article 109655. https://doi.org/10.1016/j.envres.2020.109655

Environmental Research 187 (2020) 109655

Contents lists available at ScienceDirect

Environmental Research

journal homepage: www.elsevier.com/locate/envres

Thermal energy recovery from chlorinated drinking water distribution systems: Effect on chlorine and microbial water and biofilm characteristics

Xinyan Zhou[a,b], Jawairia Imtiaz Ahmad[b,c], Jan Peter van der Hoek[b,d], Kejia Zhang[a,*]

[a] College of Civil Engineering and Architecture, Zhejiang University, Hangzhou, 310058, Zhejiang, China
[b] Sanitary Engineering, Department of Water Management, Faculty of Civil Engineering and Geosciences, Delft University of Technology, P.O. Box 5048, 2600GA, Delft, the Netherlands
[c] Institute of Environmental Sciences and Engineering, School of Civil and Environmental Engineering, National University of Science and Technology, H-12 Sector, Islamabad, Pakistan
[d] Waternet, Korte Ouderkerkerdijk 7, 1096 AC, Amsterdam, the Netherlands

ARTICLE INFO

Keywords:
Cold recovery
Chlorine
Drinking water microbial activity
Biofilm community structure
Functional prediction

ABSTRACT

Thermal energy recovery from drinking water has a high potential in the application of sustainable building and industrial cooling. However, drinking water and biofilm microbial qualities should be concerned because the elevated water temperature after cold recovery may influence the microbial activities in water and biofilm phases in drinking water distribution systems (DWDSs). In this study, the effect of cold recovery on microbial qualities was investigated in a chlorinated DWDS. The chlorine decay was slight (1.1%–15.5%) due to a short contact time (~60 s) and was not affected by the cold recovery ($p > 0.05$). The concentrations of cellular ATP and intact cell numbers in the bulk water were partially inactivated by the residual chlorine, with the removal rates of 10.1%–16.2% and 22.4%–29.4%, respectively. The chlorine inactivation was probably promoted by heat exchangers but was not further enhanced by higher temperatures. The higher water temperature (25 °C) enhanced the growth of biofilm biomass on pipelines. Principle coordination analysis (PCoA) showed that the biofilms on the stainless steel plates of HEs and the plastic pipe inner surfaces had totally different community compositions. Elevated temperatures favored the growth of *Pseudomonas* spp. and *Legionella* spp. in the biofilm after cold recovery. The community functional predictions revealed more abundances of five human diseases (e.g. *Staphylococcis aureus* infection) and beta-lactam resistance pathways in the biofilms at higher temperature. Compared with a previous study with a non-chlorinated DWDS, chlorine dramatically reduced the biofilm biomass growth but raised the relative abundances of the chlorine-resistant genera (i.e. *Pseudomonas* and *Sphingomonas*) in bacterial communities.

1. Introduction

Fossil fuels have made up the majority part of the energy resources worldwide in the past decades (Painter, 2020). However, the extensive use of these traditional energy sources poses lots of environment issues, such as global warming (Lelieveld et al., 2019). In 2015, the United Nations Paris Climate Conference reached a consensus that the global temperature rise should be well below 2 °C and efforts should be pursued to limit it to 1.5 °C (Painter, 2020; Rogelj et al., 2016). Therefore, in order to achieve this target, the pursuit of new and clean low-carbon energy resources is necessary (Jiang et al., 2010). Recently energy recovery from the water cycle has been suggested, including thermal energy from surface water, groundwater, wastewater and drinking water (Mol et al., 2011;van der Hoek, 2012a). With respect to surface water, energy recovery has already been successfully applied in practice. In the Netherlands, the water from lake "Ouderkerkerplas" is used for office building cooling, and a reduction of greenhouse gas emissions of nearly 20 kton carbon dioxide (CO_2)-equivalent/a can be achieved (van der Hoek et al., 2018). In many European countries, groundwater plays a role in the underground thermal energy storage systems and is widely used at full scale (Sanner et al., 2003). In the urban water cycle, heat recovery from wastewater via heat exchangers has been intensively studied (Elias Maxil, 2015; Elías-Maxil et al., 2014), and shower water has also been applied for heat recovery from wastewater in a pilot study (Deng et al., 2016). Recently, the concept of thermal energy recovery from drinking water has been proposed, and researchers have proven its possibility (Bloemendal et al., 2015) and explored the potential technologies in practical use (De Pasquale et al.,

* Corresponding author.
E-mail address: zhangkj@zju.edu.cn (K. Zhang).

https://doi.org/10.1016/j.envres.2020.109655
Received 23 March 2020; Received in revised form 9 April 2020; Accepted 8 May 2020
Available online 15 May 2020
0013-9351/

2017; Guo and Hendel, 2018; van der Hoek et al., 2018). However, its application still has a long way to go due to several risk concerns (Hofman and van der Wielen, 2015). The most important one is the microbial risk concern of the water quality. Because of the heat exchange, the water temperature in drinking water distribution system (DWDS) will experience an elevation, which may pose effects on microbiological growth and activity in both bulk water and biofilms (Hallam et al., 2001; van der Wielen and van der Kooij, 2010). In our previous study, such effects were evaluated in a pilot-scale non-chlorinated DWDS (Ahmad et al., 2020). However, no research has been conducted in a chlorinated one.

As a key influencing factor in DWDS, temperature can affect both chemical and biological processes (Li et al., 2019). Chlor(am)ine decay rate can be accelerated with increasing temperature (Monteiro et al., 2017; Sathasivan et al., 2009). This can be explained by two major reasons: (i) chlor(am)ine self-decay is a temperature dependent reaction, and the reaction rate is higher at higher temperature (Monteiro et al., 2017); (ii) elevated temperature can change the microbial activities (Ndiongue et al., 2005). Additionally, the efficiency of chlorine disinfection is quite sensitive to temperature (Benarde et al., 1967; Butterfield et al., 1943; Collins, 1955). Collins (1955) studied the chlorine disinfection on a chlorine-resistant species *Pseudomonas fragi*, and found that for equal destruction of *P. fragi* at 4.4 °C and 21 °C, approximately twice as much time was required at 4.4 °C. In another *Mycobacteria gordonae* inactivation study, the chlorine disinfection efficiency doubled when reaction temperature rose from 4 °C to 16 °C, and dramatically increased eight-fold when temperature reached 25 °C (Le Dantec et al., 2002). The microbial water quality in DWDS can be affected by water temperature (Blokker et al., 2013; van der Hoek, 2012b). It has been documented that seasonal temperature changes can result in fluctuations of microbial quantities (e.g. adenosine triphosphate (ATP), heterotrophic plate count, total cell count (TCC) and coliform) (LeChevallier et al., 1996; Prest et al., 2016; van der Wielen and van der Kooij, 2010) and changes of bacterial community dynamics (Pinto et al., 2014) of bulk water. Some researchers have reported that specific opportunistic pathogens favor to be present at relatively higher water temperatures (Dai et al., 2018; van der Wielen and van der Kooij, 2013). Apart from microbes in water phase, biofilm growth in DWDS can also be promoted by high temperatures (Fish et al., 2016). Tsvetanova and Dimitrov (2012) reported that significant correlations between biofilm HPC density and water temperature were detected in plastics pipes. Hallam et al. (2001) found that biofilm activity was approximately 50% lower at a temperature of 7 °C than at 17 °C. In a recent study, differences in both bacterial and fungal community compositions at two different temperatures (16 °C and 24 °C) were observed at family level (Preciado et al., 2019). In conclusion, temperature can regulate various reactions within DWDS.

In our previous study, the effect of cold recovery (with subsequent sudden temperature rise in the distributed drinking water) on microbial characteristics in both water and biofilms were investigated (Ahmad et al., 2020). However, the results were obtained through a non-chlorinated pilot DWDS. As chlorine is still widely used in drinking water disinfection worldwide, a similar study associated with thermal energy recovery is necessary in a chlorinated DWDS. Therefore, the aim of this study is to explore the effect of temperature increase on chlorine, chlorine disinfection and microbial characteristics in a pilot-scale chlorinated DWDS subjected to cold recovery. Specifically, chlorine decay, bulk water microbial activity, biofilm community structure (diversity and composition) and functional profiles of the community were investigated under the influence of cold recovery. The results could promote a better understanding of the effect of cold recovery on microorganisms in chlorinated DWDSs.

2. Materials and methods

2.1. Chemicals

Sodium hypochlorite (NaClO, 60–185 g active chlorine L^{-1}) was purchased from BOOM Lab, the Netherlands. Sodium acetate (NaAc) (500 g) was obtained from Honeywell Research Chemicals, USA. Sodium thiosulfate ($Na_2S_2O_3$) solution (0.1 N) was from Merck KGaA, Germany. Phosphate buffer solution (PBS) tablet was purchased from ThermoFisher Scientific, Sweden.

2.2. Experimental set-up

As displayed in Fig. S1 (Supplementary material), the pilot chlorinated system operated in the laboratory of Delft University of Technology consisted of a chemical dosing subsystem (CDS) and three parallel pipelines, which were (i) an experimental pipeline with an operational heat-exchanger (OHE) (Pipe1), (ii) a reference pipeline with a non-operational heat-exchanger (NOHE) (Pipe2), and (iii) a reference pipeline without a HE (Pipe3). The detailed information about the two HEs and the reason of setting two reference pipelines have been discussed in our previous study (Ahmad et al., 2020). The set-up was supplied with drinking water from the treatment plant "Kralingen" of drinking water utility Evides, Rotterdam, the Netherlands, and subsequently dosed with NaClO solution and NaAc solution (appropriate AOC supplement). This was necessary because in the Netherlands hygienically safe and biologically stable drinking water is produced, without a residual disinfectant and with a very low AOC concentration, below 10 μg acetate C L^{-1} (van der Kooij et al., 1995; Smeets et al., 2009). In the CDS (Fig. S1), NaClO stock solution (80–90 g Cl_2 L^{-1}) and NaAc stock solution (~45 mg acetate C L^{-1}) were separately dosed by two peristaltic pumps (Watson-Marlow 504U IP55 Washdown Peristaltic Pump) at a rate of 12 mL min^{-1}. At the dosing point, the theoretical chlorine concentration in the bulk water was 0.1 mg Cl_2 L^{-1}, which is the normal concentration of the residual chlorine in practical DWDSs. Due to the low AOC concentration (< 2 μg acetate C L^{-1}) in Dutch drinking water (Ahmad et al., 2019), AOC should be supplemented to mimic the production of biological not stable water in order to avoid limited microbial growth rates on the pipe surface. Thus, according to the relationship between chlorine and AOC displayed in a previous study (Ohkouchi et al., 2013), the AOC concentration in the experimental bulk water was set 50 μg acetate C L^{-1} by dosing NaAc. In order to completely mix the dosed chemicals and feed water, a static mixer (Stock Schedule 80 Threaded PVC Mixer, Koflo Corporation, USA) was installed at the main pipe before the three parallel pipelines. Each parallel pipeline, made of polyvinyl chloride-unplasticised (PVC–U), had an internal diameter of 25 mm and a length of 10 m. For this experiment, the flow rate was set at 3.3–3.8 L min^{-1} (0.11–0.13 m/s), which is within normal flow velocities in Dutch DWDSs. In Pipe 1, the water temperature after the OHE was elevated to 25 °C (the maximum admissible drinking water temperature as mentioned in the Dutch drinking water decree (State Journal, 2011)). All the pipelines were equipped with temperature and flow sensors (Fig. S1), to monitor the flow and temperature of bulk water. Dasy Lab software (version 13.0.1) was used for system monitoring and data logging.

2.3. Sampling

For water sampling, small PVC-U taps were installed in each pipeline (Fig. S1): one was at the front side (P1B, P2B or P3B) and one was at the back side (P1A, P2A or P3A). The water residence time from the front to the back sampling points was around 60 s. Feed water and water samples from six taps were taken every seven days during the experimental period (2019 March 15th to 2019 August 9th, the data of 6th, 7th, 9th week were missing). At each tap, after flushing the water for 10 s, 100 mL of water was collected for chlorine determination, and

1 L of water was collected in a sterile glass bottle containing adequate $Na_2S_2O_3$ (quenching residual chlorine) for microbial assay.

For biofilm sampling, 25 cm long PVC-U coupons (pipe sections with valves on both ends) were designed and inserted at the end part of each pipeline. At each biofilm sampling time (1st, 2nd, 3rd, 4th, 7th, 13th week), biofilms were sampled backwards from the end (p1A, p2A and p3A) of each pipeline in duplicate; and at 21st week, biofilms from both the front sides (p1B, p2B and p3B) and back sides ((p1A, p2A and p3A) of all pipelines were sampled in duplicate and in quadruplicate (two for biomass quantification and two for DNA sequencing), respectively. The two HEs were also disassembled for biofilm collection. To detach the biofilm from the coupons, pipe sections were filled with sterile PBS, placed in a water bath (Ultrasonic 8800, Branson, USA) and treated by ultra-sonication at a frequency of 40 kHz for 2 min. The biofilms grown on the inside plates of each HE were collected in a similar way. The PBS containing detached microbes were subjected to microbial analysis.

2.4. Chemical and microbial analysis

2.4.1. Aquatic chemical analysis

Free chlorine was determined by a chlorine cuvette test kit (LCK 310, HACH LANGE, Germany) and a photometer (DR 3900, HACH LANGE, Germany). Total organic carbon (TOC) was analyzed by a TOC analyzer (TOC-V CPH, SHIMADZU, Japan). pH was determined by a portable pH meter (Multi 3420, WTW, Germany) with a pH-Electrode (SenTix® 940).

2.5. Biomass quantification

Bacterial active biomass and cell numbers were quantified by measuring adenosine triphoshpate (ATP) concentration and cell counts of both water samples and biofilm samples (through the PBS containing detached microbes). For water samples, cellular ATP (cATP) concentration was determined to reflect the active biomass using a reagent kit for cATP (QGA™, Luminultra, Canada) and a luminometer (PhotonMaster™, Luminultra, Canada), while to quantify biofilm active biomass, total ATP (tATP) was determined using a reagent kit for tATP (QG21W™, Luminultra, Canada) instead. Cell counts were detected by a flow cytometer (C6-Flowcytometer, Accuri Cytometers, USA) using the same protocol that was previously developed and tested for drinking water samples (Prest et al., 2013). TCC and intact cell counts (ICC) were simultaneously distinguished by adding two stains (SYBR Green I and propidium iodide) as described by Prest et al. (2013).

2.6. DNA sequencing and bioinformatics analysis

2.6.1. DNA extraction and 16 S rRNA genes sequencing

Each PBS containing biofilm sample was filtered by a vacuum pump through a 0.22 μm polycarbonate membrane (25 mm in diameter) to collect biomass for DNA extraction. The total DNA was extracted from the membranes with a FastDNA® SPIN Kit for Soil (Mpbio, Santa Ana, California, USA) according to the manufacturer's protocol. The concentration and purity of the total DNA were measured by a NanoDrop NC2000 spectrophotometry (Thermo Fisher Scientific, Wilmington, Delaware, USA).

Primers 338F (5′-ACTCCTACGGGAGGCAGCA-3′) and 806R (5′-GGACTACHVGGGTWTCTAAT-3′) were used to amplify V3 and V4 regions of 16S rRNA gene. PCR amplification was performed using a ABI 2720 PCR (Applied Biosystems, Foster City, California, USA) with a total volume of 25 μL containing 5 μL of 5 × reaction buffer, 5 μL of 5 GC buffer, 2 μL of dNTP (2.5 mM), 1 μL of forward primer (10 μM), 1 μL of reverse primer (10 μM), 2 μL of DNA template, 8.75 μL of ddH2O, 0.25 μL of Q5 DNA polymerase. Thermal cycling conditions were as follows: an initial denaturation at 98 °C for 2 min, and 25–30 cycles at 98 °C for 15 s, 55 °C for 30 s, and 72 °C for 30 s, with a final extension at 72 °C for 5 min. Following amplification, PCR products were purified by VAHTSTM DNA Clean Beads (Vazyme, Nanjing, China), and then quantified using a microplate reader (BIOTEK-FLX800, USA). The high-throughput gene sequencing was performed on the Illumina MiSeq platform by Personal Biotechnology, Co., Ltd. (Shanghai, China).

2.6.2. Data analysis and functional prediction

Raw sequence data were quality filtered and analyzed using QIIME 2 (version 2019.4). Reads were processed by removing tags and primers, and the reads with an average quality score < 20 and read lengths < 150 bp were discarded. After being processed, reads were assembled by FLASH v 1.2.7 with the overlap between R1 and R2 reads > 10 bp. High-quality representative sequences for each operational taxonomic units (OTUs) were assigned using UCLUST with 97% sequence identity. Taxonomic classification was carried out using Greengenes 16S rRNA gene database Release 13.8 (DeSantis et al., 2006). Relative abundance (%) of individual taxa within each community was calculated by comparing the number of sequences of a specific taxon versus the number of total sequences. Alpha diversity of each microbial community was estimated based on Chao1 and Simpson index, respectively. Bray-Curtis dissimilarities were based on individual OTUs, and they were computed for the principal coordinates analyses (PCoA) using PAST 3. The functional profiles of microbial communities were predicted by using PICRUSt2 (Douglas et al., 2019) from the OTUs of 16S rRNA gene sequences, and the KEGG (Kyoto Encyclopedia of Genes and Genomes) database was employed to analyze the metabolic pathway.

2.7. Statistical methodologies

The paired T test was used to determine the significant difference of chlorine, TCC and ICC from the front and the back sampling point of each pipeline. The Wilcoxon signed-rank test was performed to determine the significant difference of cATP from the front and the back sampling point of each pipeline. The Friedmand test was used to determine the significant difference of water quality parameters from different pipelines. Pearson analysis was used to determine the correlation between cATP reduction and chlorine demand. The significant level was set as $p = 0.05$.

3. Results

3.1. Bulk water

3.1.1. Chemical parameters and temperature of feed water

During the experimental period, the pH and TOC of the feed water were within the normal value ranges (7.6 ± 0.2 and 3.0 ± 0.7 mg/L, respectively) as displayed in Table S1. As shown in Fig. 1(a), the feed water temperature was 9.3 °C at the start of the experiment and increased steadily to 21.4 °C at the end of the experiment, resulting in a temperature difference (ΔT) in Pipe 1 (the system with cold recovery with a set point of 25 °C after cold recovery) ranging from 3.6 to 15.7 °C. Thus, it can be inferred that the long-term temperature gap in Pipe1 might cause potential microbial difference of bulk water and biofilms at P1A.

3.1.2. Free chlorine

As shown in Fig. 1(b), chlorine experienced slight decreases between two sampling points in all pipelines (1.1%–15.5%). However, paired T-test showed no significant difference of chlorine concentration in Pipe1 and Pipe2 with HEs ($p > 0.05$), and significant difference ($p < 0.05$) only in Pipe3 without a HE. Also, the Friedmand test conducted at the end point of three pipelines showed no significant difference ($p > 0.05$), indicating the residual chlorine at P1A, P2A and P3A were similar. Furthermore, the chlorine demand (chlorine

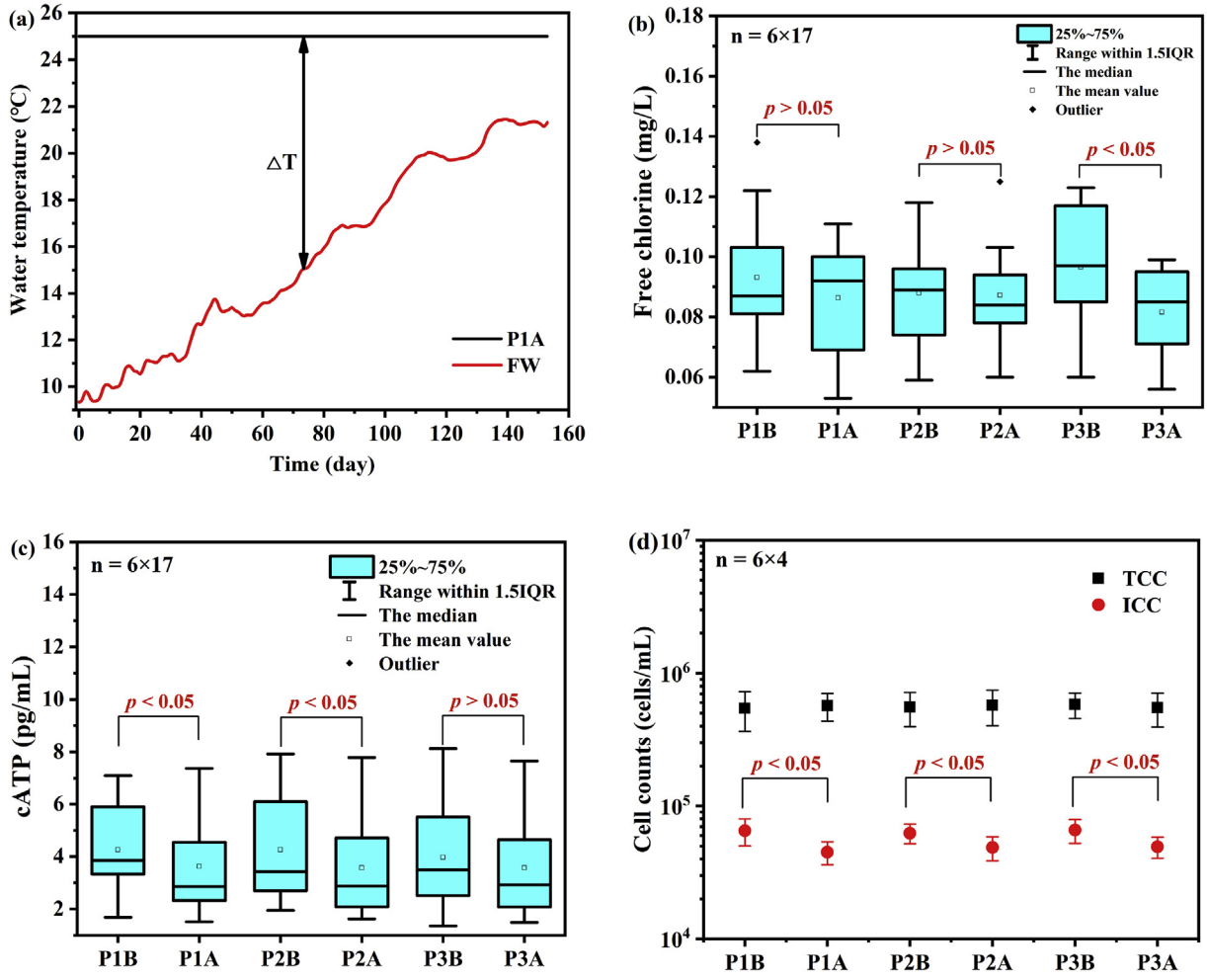

Fig. 1. (a) Feed water temperature, (b) free chlorine, (c) cATP and (d) cell counts of bulk water samples.

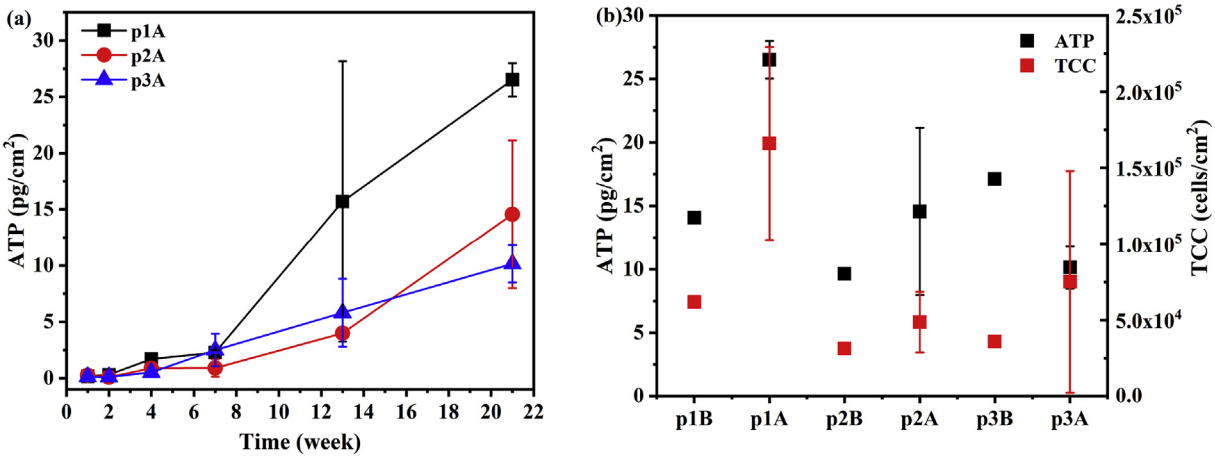

Fig. 2. Biofilm growth at (a) the back part of three pipelines and (b) comparison of biofilm biomass at week 21 among six sampling points.

concentration difference of two sampling points, PA and PB) did not display notable regularity with the change of time in both three pipes (Fig. S2).

3.1.3. Biomass

The microbial activity in the feed water reflected by cATP showed an increasing trend during the experiment from 3.11 to 6.47 pg mL^{-1} (Table S1), which was in accordance with the variation patterns of cATP at three front points P1B, P2B and P3B (Fig. S3). Fig. 1(c) showed cATP reductions in all three pipes, but only Pipe1 and Pipe2 showed significant differences ($p < 0.05$) according to the Wilcoxon signed-rank test. Additionally, the cATP concentration decrease in Pipe1 (0.63 pg mL^{-1}) and Pipe2 (0.69 pg mL^{-1}) were both higher than that in Pipe 3 (0.40 pg mL^{-1}). The results showed that the decrease of microbial activity caused by chlorine was more obvious in the two pipes with HEs, but no significant difference could be found between Pipe1

and Pipe2. Moreover, Pearson correlation analysis did not show positive correlation between cATP reduction and chlorine demand ($p > 0.05$).

As shown in Fig. 1(d), there was no significant difference ($p > 0.05$) in TCC among all samples with a narrow average concentration range of 5.51–5.81 $\times 10^5$ cells mL^{-1}. Conversely, ICC showed significant decreases in all three pipelines ($p < 0.05$), and the average reduction rates in Pipe1, Pipe2 and Pipe3 were 29.4%, 24.7% and 22.4%, respectively. However, the ICC reductions showed no significant differences among the three pipes ($p > 0.05$).

3.2. Biofilm

3.2.1. Biomass growth

The biofilm biomass growth of the back parts of three pipelines was monitored during the whole experiment. As can be seen from Fig. 2(a), the biofilm biomass increased slightly to the values of 0.91–2.49 pg cm^{-2} during the first 7 weeks, and no significant difference could be found among three pipelines. However, after 7 weeks the biomass rose dramatically in all biofilms, especially for p1A where the biofilm developed at a relatively high temperature of 25 °C. At week 21, the biofilm biomass of p1A, p2A and p3A were 26.5 ± 1.5 ATP pg cm^{-2}, 14.6 ± 6.6 ATP pg cm^{-2} and 10.2 ± 1.7 ATP pg cm^{-2}, respectively. Additionally, the final biofilm biomass reflected by both ATP and TCC (Fig. 2(b)) showed that the obvious difference between the front and the back biofilm could only be found in Pipe1 (p1B (14.8 ATP pg cm^{-2}; 6.2 $\times 10^4$ cells cm^{-2}) vs. p1A (26.5 ± 1.5 ATP pg cm^{-2}; 1.7 $\times 10^5$ cells cm^{-2})).

3.2.2. Bacterial community

In order to explore the bacterial community of different biofilm samples, high-throughput sequencing based on 16S rRNA gens was used. The results of p1A, p2A and p3A were shown as the average values of the duplicate samples, while results of OHE and NOHE were presented as single sample.

Two alpha diversity indices including Chao1 (species richness estimator) and Simpson (species diversity index) were used to analyze the biodiversity of the bacterial communities (Fig. S4(a)). p3A biofilm had the highest Chao1 and Simpson indices, indicating the highest community richness and evenness among all pipeline biofilms. p1A biofilm showed higher community richness than p2A biofilm, while its community diversity was lower than the latter one. Regarding HE samples, the Chao1 index of OHE was less than half of the value of that of NOHE. However, the Simpson index of OHE was more than twice of that of NOHE. This indicates, although the OHE biofilm community had a lower species number compared to NOHE, its species were distributed more evenly. PCoA on the OTU level were plotted to compare the bacterial community compositions of different biofilm samples (Fig. S4(b)). It is clearly shown from the plot that p1A, p2A and p3A biofilms were clustered in one group while the Bray-Curtis distances of NOHE and OHE biofilms were both far away from the pipeline group as well as from each other.

The major bacterial phylum and genus in each biofilm sample are shown by bar plots in Fig. 3. At the phylum level, *Proteobacteria* (75.6%-87.%) were dominant in all samples, followed by *Bacteroidetes* (3.6%–15.3%) and *Planctomycetes* (0.3%–4.8%). At the genus level, the top three genera in all biofilm communities were *Pseudomonas*, *Sphingomonas* and *Sphingobium*. Regarding the pipe samples, *Pseudomonas* and *Sphingobium* were found to be more abundant in p1A biofilm (20.2% and 17.4%, respectively) compared to p2A biofilm (2.9% and 5.3%, respectively) and p3A biofilm (2.7% and 12.8%, respectively). The other major genera with the highest relative abundance in p1A biofilm were *Methyloversatilis* (4.4%), *Rhizobacter* (2.7%), *Novosphingobium* (2.3%) and *Legionella* (0.14%). As for the HE samples, OHE biofilm had more *Pseudomonas* (17.3%), *Ralstonia* (7.2%) and *Vibrionimonas* (13.4%) than NOHE biofilm (2.0%, 7.2% and 4.4% for *Pseudomonas*, *Ralstonia*, and *Vibrionimonas*, respectively).

3.2.3. Functional profiles

The overall functional profiles of the bacterial communities in all biofilms were investigated based on OTU information using PICURSt2 (Fig. S5). The nearest sequenced taxon index (NSTI) of the samples were all smaller than 2, which revealed the accuracy of each prediction by calculating the sum of the phylogenetic distances for each organism in the OTU table to its nearest relative with a reference genome. A total of 176 KEGG pathways were identified, and belonged to six level 1 categories including cellular processes, environmental information processing, genetic information, human diseases, metabolism and organismal systems.

As the dominant level 1 pathway, metabolism includes several important level 2 classes associated with microbial cell growth, such as carbohydrate metabolism, amino acid metabolism and glycan biosynthesis and metabolism (Fig. S5(e)). As for the specific pathways, only three amino acid-related ones including those for tyrosine, arginine and proline, and lysine were found higher in p1A biofilm than the other two pipe biofilms (Fig. 4(a)). Fig. 4(b) shows the abundance of several commonly-studied pathways related to biofilm containing human diseases, antibiotic resistance and oxidative stress resistance. A total of 14 human diseases-related pathways were discovered and five of them (hypertrophic cardiomyopathy, epithelial cell signaling in *Helicobacter pylori* infection, *Staphylococcus aureus* infection, African trypanosomiasis and Alzheimer disease) were found both higher in p1A (among three pipeline samples) and OHE (between two HE samples). Six antibiotic biosynthesis-associated pathways and one antibiotic resistance-associated pathway were revealed, but only beta-lactam resistance was present more abundant in biofilms of both p1A and OHE. As a common oxidative stress resistance pathway, glutathione (GSH) metabolism was discovered in all biofilm samples with high abundance (Fig. 4(b)). As shown in Fig. S6, the abundances of three dominant enzymes in GSH metabolism pathway followed an order of GSH-S-transferase > GSH-peroxidase > GSH-reductase. However, only GSH-peroxidase's abundance was slightly higher in p1A and OHE biofilms.

4. Discussion

4.1. Bulk water

Due to the important role residual chlorine plays in controlling microbial regrowth in DWDS, its decay should be carefully investigated. The rate of chlorine decay has been shown to be sensitive to water temperature. Ndiongue et al. (2005) reported that in a simulated DWDS reactor, chlorine demand could rise from 0.5 Cl_2 mg L^{-1} to 1.1 Cl_2 mg L^{-1} when temperature increased from 6 °C to 18 °C. In another study (Monteiro et al., 2017), authors also proved that the reaction rate coefficient of chlorine decay increased significantly from a water temperature of 10 °C–30 °C. Additionally, the wall decay coefficient (the rate of wall chlorine decay in pipeline) showed to be related to the specific surface area (SSA) of DWDS (i.e. the pipe-wall area per unit of pipe volume) (Rossman et al., 1994; Vasconcelos and Boulos, 1996), which reasonably leads to a hypothesis that the increasing SSA brought by the HE in the two HE-installed pipelines of this study may affect the reaction rate of chlorine decay. However, the results obtained in this study showed limited chlorine decay in our set-up, and the difference of the decay in three pipelines could not be distinguished clearly as well (Fig. 1(b)). In the previous studies associated with chlorine decay, detectable chlorine concentration reduction was monitored by minutes or hours, but in our experiments the contact time of chlorine and bulk water as well as pipe wall was only ~60 s, which resulted in a slight chlorine decay and insignificant difference among different pipelines.

The detectable decreases of cATP (Fig. 1(c)) and ICC (Fig. 1(d)) in each pipe demonstrated that the chlorine level (0.1 mg Cl_2/L) in this

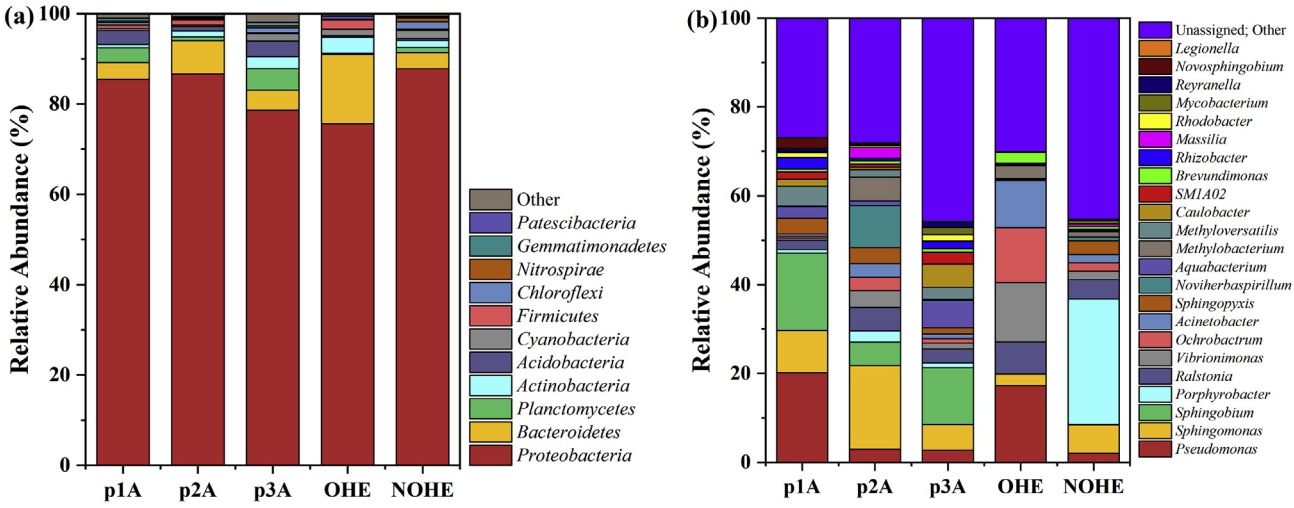

Fig. 3. Bacterial community compositions of biofilm samples at (a) phylum level and (b) genus level.

study could partially inhibit the microbial activity in the bulk water within a short contact time. However, such inhibition showed no obvious difference between Pipe1 and Pipe2, indicating limited effect of sudden temperature increase on the chlorine inactivation. The disinfection rate of chlorine is temperature-dependent as discussed above. Nevertheless, as with the absence of a temperature effect on chlorine decay, the absence of a temperature effect on microbial inactivation in this study could also be explained by the short contact time. It should be noted that the pipelines with HE showed larger microbial reduction (Fig. 1(c)) than Pipe3 (without HE). It may be hypothesized that a HE could enhance the disinfection efficiency of chlorine towards microbes, although this could not be confirmed by a chlorine demand increase in this study. A possible explanation for the enhanced disinfection efficiency may be that the closely-aligned plates designed for increasing heat-exchange efficiency in the HE provided several micro-channels for the water flowing through the HE, which enhanced the mixing efficiency of the potential reactants (Li et al., 2007). This might improve the contact frequency between chlorine and microorganisms and subsequently result in a promotion of disinfection efficiency. However, the actual mechanism should be further investigated.

4.2. Biofilm

In this study, each pipeline biofilm underwent a “lag time”, when biomass increased slowly on the pipe surface. This is consistent with a previous study, where detectable biomass was present on the 40th day after the beginning of biofilm formation (Wang et al., 2019). In the lag time, reversible and irreversible attachment of microbial cells successively happen on the pipe surface before the cell proliferation (Liu et al., 2016). Our results showed a much faster biomass growth rate of the biofilm at a higher constant temperature (25 ˚C) than the ones in the lower fluctuating temperatures (13.3–21.3 ˚C) after the lag time (Fig. 2(a)). This finding is in accordance with the previously obtained conclusion that an elevated temperature increases biofilm growth, especially in the presence of biodegradable organic matter (Hallam et al., 2001; Tsvetanova and Dimitrov, 2012). Within the common water temperature range, the increase of temperature can promote the microbial cell secretion of extracellular polymeric substances (EPS), a key substance for the microbial early aggregate on the pipe surface (Herald and Zattola, 1988; Yu et al., 2019), and enhance the activity and growth rate of the attached cells (Mayo and Noike, 1996). In contrast, Ndiongue et al. (2005) and Ollos (1998) reported that the temperature effect on biofilm growth became limited when biofilms were in a steady state. Therefore, it can be hypothesized that the biofilm biomass of p2A and p3A might have been closer to that of p1A if the biofilm growth time was long enough to reach a steady state.

Alpha diversity analysis revealed that due to the higher temperature (approximate 27 ˚C) of the OHE's wall surface than that of NOHE's (Ahmad et al., 2020), the biofilm of OHE had less diverse but more stable community composition than NOHE, which was rewarding to maintain the water quality after the cold recovery. PCoA analysis showed that the community compositions of p1A, p2A and p3A clustered in one group (all on PVC-U surface), compared to OHE and NOHE (both on 316 stainless steel (SS) surface), indicating surface material could shape the biofilm community structure. This could be supported by the former studies which confirmed that pipe materials could affect the diversity and composition of the biofilm community (Norton and LeChevallier, 2000; Yu et al., 2010). The investigation of community composition showed much higher *Pseudomonas* proportion in the biofilms developing in the higher temperatures (p1A and OHE). It has been reported that *Pseudomonas* spp. favors growing in warmer water under oligotrophic conditions (Proctor et al., 2017). The temperature gap between warm samples (p1A and OHE) and cold samples (p2A, p3A, NOHE) might result in the predominance of *Pseudomonas* in the warm samples. Additionally, the relative abundances of other genera like *Sphingobium*, *Novosphingobium*, *Methyloversatilis*, *Ralstonia* and *Legionella* were also found higher in warmer biofilms (p1A or OHE), and all of them were previously discovered as major inhabitants in the warm environments like hot pipes or geothermal springs (Farhat et al., 2018; Jiang et al., 2016; Mahato et al., 2019; van der Kooij et al., 2017). Because of the likely pathogenic risks brought by *Pseudomonas* and *Legionella* (Hwang et al., 2007), their higher proportions in the biofilms during and after the cold recovery should be heeded.

The community functional predictions revealed that five human diseases-associated pathways were more abundant in warmer biofilms. Among them, *Staphylococcus aureus* infection is a common waterborne infection-related gene function (Li et al., 2020), which could be attributed to the presence of genus *Staphylococcus* in the biofilms, although it was not abundant in warmer biofilms. Several functional pathways related to antibiotic resistance and biosynthesis were discovered, however, only the pathway for beta-lactam resistance was obviously abundant in both P1A and OHE biofilms. The existence of ARGs were previously found in DWDSs (Xu et al., 2016), and their concentrations or compositions could be affected by water temperature (Li et al., 2018; Liu et al., 2018). The high abundance of beta-lactam resistance in the warmer samples here might be explained by the dominance of genus *Pseudomonas*, some species of which were documented to be the host of beta-lactam resistance genes (Torrens et al., 2019). The pathway of GSH metabolism, a typical mechanism for protecting cell from oxidative damage (Douterelo et al., 2018), was

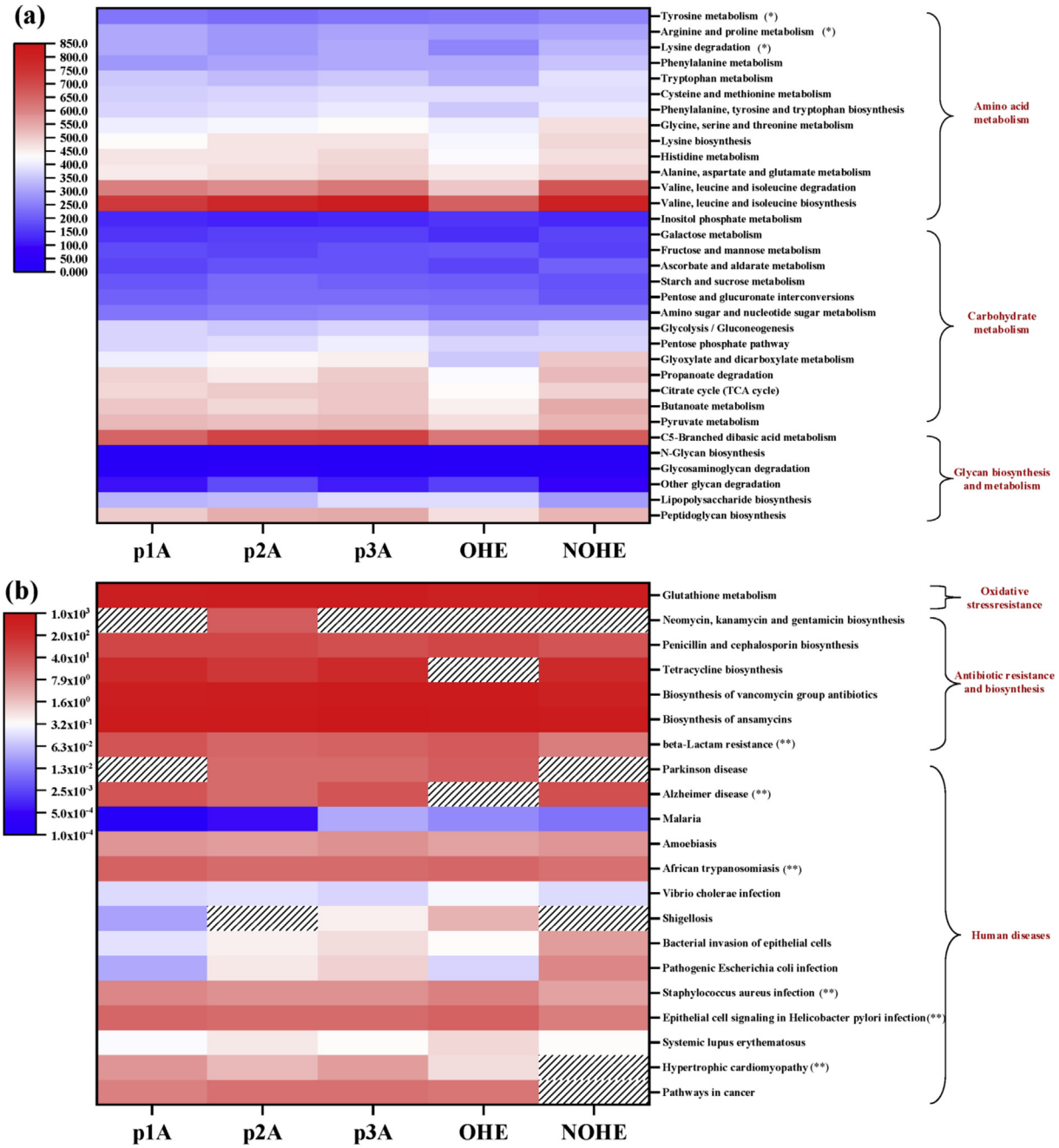

Fig. 4. Heat map of KEGG pathways for the abundance of (a) metabolism associated with cell growth and (b) other important pathways ("*" refers to the abundance which is the highest in p1A biofilm compared to other two pipeline biofilms; "**" refers to the abundance which is not only the highest in p1A biofilm among pipeline biofilms, but also higher in OHE biofilm between HE samples; "slash" represents "0" in abundance).

discovered abundantly in all samples. This is reasonable because the residual chlorine in the bulk water could stimulate the synthesis of GSH: GSH-reductase reduced the disulphide of GSH to sulfhydryl (Kehrer et al., 2010), which played an important role in resisting oxidative stress of free chlorine. However, the temperature difference did not significantly affect the abundance of the key enzymes involved in GSH synthesis.

4.3. Comparison between chlorinated and non-chlorinated cold recovery DWDSs

In our previous study (Ahmad et al., 2020), the effect of cold recovery on the biofilm formation in a non-chlorinated system was investigated. In that study, after 38 weeks of experimental duration, 5.3 times more biofilm was formed after cold recovery (475 ATP pg cm^{-2}) compared to biofilm formed without cold recovery (89 ATP pg cm^{-2}). However, in the present chlorinated DWDSs, the biofilm biomass after 21 weeks with and without cold recovery was only 26.5 ATP pg cm^{-2} and 14.6 ATP pg cm^{-2}, respectively. This means the biofilm biomass was much lower in the chlorinated system than the non-chlorinated system. Although the total biofilm forming time of the previous study was nearly twice (21 weeks vs. 38 weeks) of that of this study, this could not explain 6 to 18 times more biomass in the former case than this one. Therefore, the main reason for this massive difference could be attributed to the negative effect of chlorine on the biofilm formation. The presence of chlorine could degrade the bacterial cell-membrane functional groups to slow down the microbial depositions onto the pipe wall and, therefore prevented the reversible to irreversible transition of

cell attachment to surfaces (Xue and Seo, 2013). Furthermore, chlorine could reduce the microbial growth rate of the attached microbes (Butterfield et al., 2002). It should be noted that the increase in biomass (the ratio of the biomass with and without cold recovery) was also hindered by chlorine in our chlorinated DWDS compared to the previous non-chlorinated one (1.8 and 5.3 times for chlorinated system and non-chlorinated system, respectively). In other words, the cold recovery effect became less obvious in the chlorinated system. This might be due to the promotion of chlorine inactivation towards biofilm when temperature increased.

Regarding the difference of the biofilm community compositions of the two studies, the chlorine-resistant bacteria (CRB) genera *Pseudomonas* and *Sphingomonas* (Butterfield et al., 2002) were more abundant in the chlorinated biofilms (2.7%–20.2% and 5.8%–18.8%, respectively) than the non-chlorinated ones (0.2%–2.3% and < 1.0%, respectively). This was in accordance with other studies which reported that the use of chlorination could lead to the selection of CRB, including several opportunistic pathogens (Ingerson-Mahar and Reid, 2012; Sun et al., 2013). Moreover, in this study the abundances of *Pseudomonas* and *Sphingomonas* were both higher in plastic pipe biofilms (*Pseudomonas*: 2.8%–20.2% and *Sphingomonas*: 9.5%–12.3%) than HE biofilms (*Pseudomonas*: 2.0%–17.2% and *Sphingomonas*: 2.5%–6.4%) under the same temperatures (Fig. 3), suggesting surface materials could also affect the abundances of CRB in biofilms. Unfortunately, due to the lack of biomass data of HE biofilm, the CRB densities on plastic pipe inner surfaces and HE SS plates could not be compared directly. However, according to a previous biofilm formation study under long-term high chlorine level (Zhu et al., 2014), the biomass density in the stabilized biofilm on SS pipe was lower than that on plastic pipes. Thus, in the consideration of both biomass and CRB abundance, SS pipe material can be recommended to prevent the proliferation of CRB in DWDSs.

4.4. Outlook for future research

Considering the experimental results obtained in this study, specific topics should attain attention in future research concerning cold recovery from chlorinated DWDSs:

(1) In order to investigate the cold recovery effect on the chlorine decay and microbial inactivation efficiency, prolonged contact time should be achieved by using experimental set-ups with longer pipelines. Also, the effect of initial chlorine concentration should be studied.
(2) The processes that take place between the plates of the HEs should be fully investigated. The interaction between chlorine and microorganisms inside the HE needs to be intensively explored. Chlorine decay inside the HE is of concern, especially for HEs after prolonged running times, when biofouling and corrosion are present on the plate surface (Murthy et al., 2005). Additionally, a proper residual chlorine level should be determined to balance microbial control and chlorine-induced corrosion on the HE plate surface (Martins et al., 2014).
(3) In this work, cATP and ICC showed a decreasing trend in bulk waters, but no quantification of specific species (e.g. pathogens) was conducted. The analysis of microbial community composition and functional prediction showed that there were relatively high risks of pathogenic, antibiotic resistance and human diseases related bacteria in the biofilms after cold recovery. As chlorine can promote the detachment of cells from biofilms (Chen and Stewart, 2000), the potential detachment of the risky bacteria should be monitored after the cold recovery where chlorine becomes more active due to the rising temperature.
(4) In this study, chlorine resulted in higher abundances of CRB in biofilms. To mitigate the risk of CRB, researchers have recently proposed several combined disinfection processes such as UV/Cl_2, UV/hydrogen peroxide, UV/peroxymonosulfate, etc. (Zhu et al., 2020; Zeng et al., 2020), although most of these processes were only explored on lab-scale. Future studies may focus on optimizing operation parameters to balance continuous disinfection ability and biofilm CRB control, and large-scale application of these technologies in the practical field.

5. Conclusions

This study explored the effect of cold recovery on the drinking water microbial quality (as cATP, TCC and ICC), and biofilm growth and composition in a chlorinated DWDSs. Slight chlorine decay was detected in all pipelines, but was not affected by the temperature increase. Chlorine could partially inactivate the microbial activities in bulk water, and the inactivation efficiency was slightly promoted by the HEs. The growth rate of biofilm biomass was significantly enhanced by water temperature. The diversity and composition of biofilm microbial community were both shaped by cold recovery and surface materials. For example, *Pseudomonas* spp. had higher abundances in warm biofilms. Metagenomics functional prediction by PICRUSt2 revealed more abundance of several pathways linked to human diseases and beta-lactam resistance were found in the biofilm after cold recovery. Compared to the previous results from a non-chlorinated DWDS, the effect of chlorine in this study led to much lower biomass but higher abundances of chlorine-resistant bacteria in the biofilms.

Funding

This work was supported by Waternet, the water utility of Amsterdam and surroundings, the Topsector Water TKI Water technology Program (grant nr. 2015TUD003) of the Dutch Ministry of Economic Affairs and Climate Change, National Natural Science Foundation of China (No. 51978602), and Major Science and Technology Program for Water Pollution Control and Treatment (No. 2017ZX07201004).

CRediT authorship contribution statement

Xinyan Zhou: Conceptualization, Methodology, Formal analysis, Data curation, Writing - original draft. **Jawairia Imtiaz Ahmad:** Writing - review & editing. **Jan Peter van der Hoek:** Writing - review & editing, Funding acquisition. **Kejia Zhang:** Funding acquisition, Supervision.

Declaration of competing interest

The authors declare that they have no known competing financial interests or personal relationships that could have appeared to influence the work reported in this paper.

Acknowledgement

The work was supported by Waternet, the water utility of Amsterdam and surroundings, the Topsector Water TKI Water technology Program (grant nr. 2015TUD003) of the Dutch Ministry of Economic Affairs and Climate Change, National Natural Science Foundation of China (No. 51978602), and Major Science and Technology Program for Water Pollution Control and Treatment (No. 2017ZX07201004).

Appendix A. Supplementary data

Supplementary data to this article can be found online at https://doi.org/10.1016/j.envres.2020.109655.

References

Ahmad, J.I., Giorgi, S., Zlatanovic, L., Liu, G., Medema, G., Van Der Hoek, J.P., September, 2019. Drinking Water Distribution Networks: an Emerging Resource for Thermal. 3rd IWA Resource Recovery Conference, Venice, Italy.

Ahmad, J.I., Liu, G., van der Wielen, P.W., Medema, G., van der Hoek, J.P., 2020. Effects of cold recovery technology on the microbial drinking water quality in unchlorinated distribution systems. Environ. Res. 183, 109175.

Benarde, M.A., Snow, W.B., Olivieri, V.P., 1967. Chlorine dioxide disinfection temperature effects. J. Appl. Bacteriol. 30 (1), 159–167.

Bloemendal, M., Moerman, A., Hofman, J., Blokker, M., Agudelo-Vera, C., 2015. Recovery of Energy from Pipes. Report BTO 2015.001, Nieuwegein, The Netherlands (In Dutch). KWR Watercycle Research Institute.

Blokker, E.J.M., van Osch, A.M., Hogeveen, R., Mudde, C., 2013. Thermal energy from drinking water and cost benefit analysis for an entire city. J. Water Clim. Change 4 (1), 11–16.

Butterfield, C.T., Wattie, E., Megregian, S., Chambers, C.W., 1943. Influence of pH and temperature on the survival of coliforms and enteric pathogens when exposed to free chlorine. Publ. Health Rep. 1837–1866 1896-1970.

Butterfield, P.W., Camper, A.K., Ellis, B.D., Jones, W.L., 2002. Chlorination of model drinking water biofilm: implications for growth and organic carbon removal. Water Res. 36 (17), 4391–4405.

Chen, X., Stewart, P.S., 2000. Biofilm removal caused by chemical treatments. Water Res. 34 (17), 4229–4233.

Collins, E.B., 1955. Factors involved in the control of gelatinous curd defects of cottage cheese: II. Influence of pH and temperature upon the bactericidal efficiency of chlorine. J. Milk Food Technol. 18 (8), 189–191.

Dai, D., Rhoads, W.J., Edwards, M.A., Pruden, A., 2018. Shotgun metagenomics reveals taxonomic and functional shifts in hot water microbiome due to temperature setting and stagnation. Front. Microbiol. 9, 2695.

De Pasquale, A.M., Giostri, A., Romano, M.C., Chiesa, P., Demeco, T., Tani, S., 2017. District heating by drinking water heat pump: modelling and energy analysis of a case study in the city of Milan. Energy 118, 246–263.

Deng, Z., Mol, S., van der Hoek, J.P., 2016. Shower heat exchanger: reuse of energy from heated drinking water for CO_2 reduction. DWES 9, 1–8.

DeSantis, T.Z., Hugenholtz, P., Larsen, N., Rojas, M., Brodie, E.L., Keller, K., Huber, T., Dalevi, D., Hu, P., Andersen, G.L., 2006. Greengenes, a chimera-checked 16S rRNA gene database and workbench compatible with ARB. Appl. Environ. Microbiol. 72 (7), 5069–5072.

Douglas, G.M., Maffei, V.J., Zaneveld, J., Yurgel, S.N., Brown, J.R., Taylor, C.M., Huttenhower, C., Langille, M.G., 2019. PICRUSt2: an Improved and Extensible Approach for Metagenome Inference. BioRxiv, pp. 672295.

Douterelo, I., Calero-Preciado, C., Soria-Carrasco, V., Boxall, J.B., 2018. Whole metagenome sequencing of chlorinated drinking water distribution systems. Environ. Sci-Wat. Res. 4 (12), 2080–2091.

Elias Maxil, J.A., 2015. Heat Modeling of Wastewater in Sewer Networks: Determination of Thermal Energy Content from Sewage with Modeling Tools. Doctoral Thesis. Department of Water Management, Delft University of Technology, Delft, the Netherlands.

Elías-Maxil, J.A., van der Hoek, J.P., Hofman, J., Rietveld, L., 2014. A bottom-up approach to estimate dry weather flow in minor sewer networks. Water Sci. Technol. 69 (5), 1059–1066.

Farhat, M., Moletta Denat, M., Trouilhé, M.C., Frère, J., Robine, E., 2018. Transitory change of bacterial community structure in hot water biofilm: effects of anti–Legionella treatments. Clean 46 (6), 1700203.

Fish, K.E., Osborn, A.M., Boxall, J., 2016. Characterising and understanding the impact of microbial biofilms and the extracellular polymeric substance (EPS) matrix in drinking water distribution systems. Environ. Sci.-Water Res. 2 (4), 614–630.

Guo, X., Hendel, M., 2018. Urban water networks as an alternative source for district heating and emergency heat-wave cooling. Energy 145, 79–87.

Hallam, N.B., West, J.R., Forster, C.F., Simms, J., 2001. The potential for biofilm growth in water distribution systems. Water Res. 35 (17), 4063–4071.

Herald, P.J., Zattola, E.A., 1988. Attachment of Listeria monocytogenes to stainless steel surfaces at various temperatures and pH values. J. Food Sci. 53 (5), 1549–1562.

Hofman, J., van der Wielen, P., 2015. Heat and Cold from Drinking Water and Sewage System. Report BTO 2015.002, Nieuwegein, The Netherlands (In Dutch). KWR Watercycle Research Institute.

Hwang, M.G., Katayama, H., Ohgaki, S., 2007. Inactivation of Legionella pneumophila and Pseudomonas aeruginosa: evaluation of the bactericidal ability of silver cations. Water Res. 41 (18), 4097–4104.

Ingerson-Mahar, M., Reid, A., 2012. Microbes in pipes: the microbiology of the water distribution system (report). Am. Acad. Microbiol. 1–28.

Jiang, Z., Li, P., Jiang, D., Dai, X., Zhang, R., Wang, Y., Wang, Y., 2016. Microbial community structure and arsenic biogeochemistry in an acid vapor-formed spring in Tengchong geothermal area, China. PloS One 11 (1).

Jiang, B., Sun, Z., Liu, M., 2010. China's energy development strategy under the low-carbon economy. Energy 35 (11), 4257–42645.

Kehrer, J.P., Robertson, J.D., Smith, C.V., 2010. 1.14 - free radicalsand reactive oxygen species. Compr. Toxicol. 1, 277–307.

LeChevallier, M.W., Welch, N.J., Smith, D.B., 1996. Full-scale studies of factors related to coliform regrowth in drinking water. Appl. Environ. Microbiol. 62 (7), 2201–2211.

Le Dantec, C., Duguet, J., Montiel, A., Dumoutier, N., Dubrou, S., Vincent, V., 2002. Chlorine disinfection of atypical mycobacteria isolated from a water distribution system. Appl. Environ. Microbiol. 68 (3), 1025–1032.

Lelieveld, J., Klingmüller, K., Pozzer, A., Burnett, R.T., Haines, A., Ramanathan, V., 2019. Effects of fossil fuel and total anthropogenic emission removal on public health and climate. Proc. Natl. Acad. Sci. Unit. States Am. 116 (15), 7192–7197.

Li, A., Chen, L., Zhang, Y., Tao, Y., Xie, H., Li, S., Sun, W., Pan, J., He, Z., Mai, C., 2018. Occurrence and distribution of antibiotic resistance genes in the sediments of drinking water sources, urban rivers, and coastal areas in Zhuhai, China. Environ. Sci. Pollut. Res. 25 (26), 26209–26217.

Li, R.A., McDonald, J.A., Sathasivan, A., Khan, S.J., 2019. Disinfectant residual stability leading to disinfectant decay and by-product formation in drinking water distribution systems: a systematic review. Water Res. 153, 335–348.

Li, S., Xu, J., Wang, Y., Luo, G., 2007. Mesomixing scale controlling and its effect on micromixing performance. Chem. Eng. Sci. 62 (13), 3620–3626.

Li, W., Tan, Q., Zhou, W., Chen, J., Li, Y., Wang, F., Zhang, J., 2020. Impact of substrate material and chlorine/chloramine on the composition and function of a young biofilm microbial community as revealed by high-throughput 16S rRNA sequencing. Chemosphere 242, 125310.

Liu, S., Gunawan, C., Barraud, N., Rice, S.A., Harry, E.J., Amal, R., 2016. Understanding, monitoring, and controlling biofilm growth in drinking water distribution systems. Environ. Sci. Technol. 50 (17), 8954–8976.

Liu, S., Qu, H., Yang, D., Hu, H., Liu, W., Qiu, Z., Hou, A., Guo, J., Li, J., Shen, Z., 2018. Chlorine disinfection increases both intracellular and extracellular antibiotic resistance genes in a full-scale wastewater treatment plant. Water Res. 136, 131–136.

Mahato, N.K., Sharma, A., Singh, Y., Lal, R., 2019. Comparative metagenomic analyses of a high-altitude Himalayan geothermal spring revealed temperature-constrained habitat-specific microbial community and metabolic dynamics. Arch. Microbiol. 201 (3), 377–388.

Martins, C., Moreira, J.L., Martins, J.I., 2014. Corrosion in water supply pipe stainless steel 304 and a supply line of helium in stainless steel 316. Eng. Fail. Anal. 39, 65–71.

Mayo, A.W., Noike, T., 1996. Effects of temperature and pH on the growth of heterotrophic bacteria in waste stabilization ponds. Water Res. 30 (2), 447–455.

Mol, S., Kornman, J.M., Kerpershoek, A.J., Van Der Helm, A., 2011. Opportunities for public water utilities in the market of energy from water. Water Sci. Technol. 63 (12), 2909–2915.

Monteiro, L., Figueiredo, D., Covas, D., Menaia, J., 2017. Integrating water temperature in chlorine decay modelling: a case study. Urban Water J. 14 (10), 1097–1101.

Murthy, P.S., Venkatesan, R., Nair, K., Inbakandan, D., Jahan, S.S., Peter, D.M., Ravindran, M., 2005. Evaluation of sodium hypochlorite for fouling control in plate heat exchangers for seawater application. Int. Biodeterior. Biodegrad. 55 (3), 161–170.

Ndiongue, S., Huck, P.M., Slawson, R.M., 2005. Effects of temperature and biodegradable organic matter on control of biofilms by free chlorine in a model drinking water distribution system. Water Res. 39 (6), 953–964.

Norton, C.D., LeChevallier, M.W., 2000. A pilot study of bacteriological population changes through potable water treatment and distribution. Appl. Environ. Microbiol. 66 (1), 268–276.

Ohkouchi, Y., Ly, B.T., Ishikawa, S., Kawano, Y., Itoh, S., 2013. Determination of an acceptable assimilable organic carbon (AOC) level for biological stability in water distribution systems with minimized chlorine residual. Environ. Monit. Assess. 185 (2), 1427–1436.

Ollos, P.J., 1998. Effects of Drinking Water Biodegradability and Disinfectant Residual on Bacterial Regrowth. Doctoral Thesis. Department of Civil Engineering, University of Waterloo, Ontario, Canada.

Painter, D.S., 2020. Review of the book burning up: a global history of fossil fuel consumption, by simon pirani. J. Interdiscip. Hist. 50 (3), 442–443. https://www.muse.jhu.edu/article/741623.

Pinto, A.J., Schroeder, J., Lunn, M., Sloan, W., Raskin, L., 2014. Spatial-temporal survey and occupancy-abundance modeling to predict bacterial community dynamics in the drinking water microbiome. mBio 5 (3) e01135-14.

Prest, E.I., Hammes, F., Kötzsch, S., Van Loosdrecht, M., Vrouwenvelder, J.S., 2013. Monitoring microbiological changes in drinking water systems using a fast and reproducible flow cytometric method. Water Res. 47 (19), 7131–7142.

Prest, E.I., Weissbrodt, D.G., Hammes, F., Van Loosdrecht, M.C.M., Vrouwenvelder, J.S., 2016. Long-term bacterial dynamics in a full-scale drinking water distribution system. PloS One 11 (10).

Preciado, C.C., Boxall, J., Soria-Carrasco, V., Douterelo, I., 2019. Effect of temperature increase in bacterial and fungal communities of chlorinated drinking water distribution systems. Access Microbiol. 1 (1A).

Proctor, C.R., Dai, D., Edwards, M.A., Pruden, A., 2017. Interactive effects of temperature, organic carbon, and pipe material on microbiota composition and Legionella pneumophila in hot water plumbing systems. Microbiome 5 (1), 130.

Rogelj, J., Den Elzen, M., Höhne, N., Fransen, T., Fekete, H., Winkler, H., Schaeffer, R., Sha, F., Riahi, K., Meinshausen, M., 2016. Paris Agreement climate proposals need a boost to keep warming well below 2 °C. Nature 534 (7609), 631–639.

Rossman, L.A., Clark, R.M., Grayman, W.M., 1994. Modeling chlorine residuals in drinking-water distribution systems. J. Environ. Eng. 120 (4), 803–820.

Sanner, B., Karytsas, C., Mendrinos, D., Rybach, L., 2003. Current status of ground source heat pumps and underground thermal energy storage in Europe. Geothermics 32 (4–6), 579–588.

Sathasivan, A., Chiang, J., Nolan, P., 2009. Temperature dependence of chemical and microbiological chloramine decay in bulk waters of distribution system. Water Sci. Technol. Water Supply 9 (5), 493–499.

State Journal, 2011. Decree of 23 May 2011 concerning the regulations for the production and distribution of drinking water and the organization of the public drinking water supply. Staatscourant - Off. J. Royal Kingdom Netherlands No. 293 23 May 2011 (in Dutch).

Sun, W., Liu, W., Cui, L., Zhang, M., Wang, B., 2013. Characterization and identification of a chlorine-resistant bacterium, *Sphingomonas* TS001, from a model drinking water

distribution system. Sci. Total Environ. 458, 169–175.
Smeets, P.W.M.H., Medema, G.J., Van Dijk, J.C., 2009. The Dutch secret: how to provide safe drinking water without chlorine in The Netherlands. Drinking Water Eng. Sci. 2 (1), 1.
Torrens, G., Hernández, S.B., Ayala, J.A., Moya, B., Juan, C., Cava, F., Oliver, A., 2019. Regulation of AmpC-driven β-lactam resistance in *Pseudomonas aeruginosa*: different pathways, different signaling. mSystems 4 (6).
Tsvetanova, Z.G., Dimitrov, D.N., 2012. Biofilms and bacteriological water quality in a domestic installation model simulating daily drinking water consumption. Water Sci. Technol. Water Supply 12 (6), 720–726.
van der Hoek, J.P., 2012a. Climate change mitigation by recovery of energy from the water cycle: a new challenge for water management. Water Sci. Technol. 65 (1), 135–141.
van der Hoek, J.P., 2012b. Towards a climate neutral water cycle. J. Water Clim. Change 3 (3), 163–170.
van der Hoek, J.P., Mol, S., Giorgi, S., Ahmad, J.I., Liu, G., Medema, G., 2018. Energy recovery from the water cycle: thermal energy from drinking water. Energy 162, 977–987.
van der Kooij, D., Bakker, G.L., Italiaander, R., Veenendaal, H.R., Wullings, B.A., 2017. Biofilm composition and threshold concentration for growth of *Legionella pneumophila* on surfaces exposed to flowing warm tap water without disinfectant. Appl. Environ. Microbiol. 83 (5), e2716–e2737.
van der Kooij, D., Drost, Y.C., Hijnen, W.A.M., Willemsen-Zwaagstra, J., Nobel, P.J., Schellart, J.A., 1995. Multiple barriers against micro-organisms in water treatment and distribution in The Netherlands. Water Supply 13–23.
van der Wielen, P.W., van der Kooij, D., 2010. Effect of water composition, distance and season on the adenosine triphosphate concentration in unchlorinated drinking water in The Netherlands. Water Res. 44 (17), 4860–4867.
van der Wielen, P.W., van der Kooij, D., 2013. Nontuberculous mycobacteria, fungi, and opportunistic pathogens in unchlorinated drinking water in The Netherlands. Appl. Environ. Microbiol. 79 (3), 825–834.
Vasconcelos, J.J., Boulos, P.F., 1996. Characterization and Modeling of Chlorine Decay in Distribution Systems. American Water Works Association, USA.
Wang, Y., Zhu, B., Tong, J., Bai, X., 2019. Growth features of water supply pipeline biofilms based on active microorganisms. Chin. J. Environ. Sci. 2 (40), 853–858 (in Chinese).
Xu, L., Ouyang, W., Qian, Y., Su, C., Su, J., Chen, H., 2016. High-throughput profiling of antibiotic resistance genes in drinking water treatment plants and distribution systems. Environ. Pollut. 213, 119–126.
Xue, Z., Seo, Y., 2013. Impact of chlorine disinfection on redistribution of cell clusters from biofilms. Environ. Sci. Technol. 47 (3), 1365–1372.
Yu, J., Kim, D., Lee, T., 2010. Microbial diversity in biofilms on water distribution pipes of different materials. Water Sci. Technol. 61 (1), 163–171.
Yu, R., Liu, Z., Yu, Z., Wu, X., Shen, L., Liu, Y., Li, J., Qin, W., Qiu, G., Zeng, W., 2019. Relationship among the secretion of extracellular polymeric substances, heat resistance, and bioleaching ability of *Metallosphaera sedula*. Int. J. of Min. Met. Mater. 26 (12), 1504–1511.
Zeng, F.Z., Cao, S., Jin, W.B., Zhou, X., Ding, W.Q., Tu, R.J., Han, S.F., Wang, C.P., Jiang, Q.J., Huang, H., Ding, F., 2020. Inactivation of chlorine-resistant bacterial spores in drinking water using UV irradiation, UV/Hydrogen peroxide and UV/Peroxymonosulfate: efficiency and mechanism. J. Clean. Prod. 243, 118666.
Zhu, Y., Chen, L., Xiao, H., Shen, F., Deng, S.H., Zhang, S.R., He, J.S., Song, C., Wang, X., Zhang, J.H., Gong, L., Hu, C., 2020. Effects of disinfection efficiency on microbial communities and corrosion processes in drinking water distribution systems simulated with actual running conditions. J. Environ. Sci-China 88, 273–282.
Zhu, Z., Wu, C., Zhong, D., Yuan, Y., Shan, L., Zhang, J., 2014. Effects of pipe materials on chlorine-resistant biofilm formation under long-term high chlorine level. Appl. Biochem. Biotechnol. 173 (6), 1564–1578.